

EXPERIMENTAL STUDIES OF A STEEL FRAME MODEL WITH AND WITHOUT BUCKLING-RESTRAINED BRACES

Héctor Guerrero ⁽¹⁾, Tianjian Ji ⁽²⁾, and José A. Escobar ⁽³⁾

ABSTRACT

This paper presents comparative experimental studies of a five-storey steel-frame model at a scale of 1/10 with, and without, buckling-restrained braces (BRBs). The building model was subjected to free vibration tests and shaking table tests. The latter were conducted using low-intensity white noise and seismic input. From the free vibration tests and shaking table tests with low-intensity white noise, it was found that the BRBs contributed a significant amount of damping. This happened to the model even at low levels of vibration. The shaking table tests with seismic input were conducted using seven earthquake records, taken in the lakebed zone of Mexico City with seismic intensities from $pga=0.1g$ to $0.25g$. At an intensity of $pga=0.1g$, the results show that the model fitted with BRBs had a significantly smaller response than the bare model, in terms of displacement, inter-storey drift, floor velocity and floor acceleration. The higher intensities were only applied to the model fitted with BRBs. The results indicate that the model with BRBs was able to withstand about 2.5 times the seismic intensity of the bare model, in terms of lateral displacement, inter-storey drift and Arias Intensity, as a measure of the energy contents of the movement. At the end of the tests, all BRBs were removed and the model remained in its original undamaged state.

Keywords: buckling-restrained braces (BRBs); free vibration tests; shaking table tests; steel-frame model; lakebed zone of Mexico City

RESUMEN

Este artículo presenta estudios experimentales en un marco de acero de cinco niveles, a escala natural de 1/10, con y sin contraventeos restringidos al pandeo (CRP). El modelo fue sometido a pruebas de vibración libre y en mesa vibradora. Estas últimas se realizaron con movimientos a base de ruidos blancos de baja intensidad y con movimientos sísmicos. De las pruebas de vibración libre y de mesa vibradora con ruidos blancos se encontró que los CRP incrementaron de manera muy importante el nivel de amortiguamiento en el modelo. Esto sucedió aun cuando el modelo se sometió a niveles de vibración baja que no generaron respuesta no lineal. Para las pruebas con movimientos sísmicos se utilizaron siete acelerogramas registrados en la zona del lago de la Ciudad de México, escalados a intensidades entre $pga=0.1g$ y $0.25g$, siendo pga la aceleración máxima de piso y g la aceleración de la gravedad. A la intensidad de $pga=0.1g$, los resultados muestran que el modelo equipado con CRP tuvo una respuesta mucho menor al caso sin CRP; esto en términos de desplazamientos, distorsión de entrepiso, velocidad y aceleraciones de piso. Las intensidades mayores fueron sólo aplicadas en el modelo con CRP. Los resultados indican que el modelo con CRP pudo acomodar hasta 2.5 veces más

Artículo recibido el 17 de diciembre de 2015 y aprobado para su publicación el 7 de diciembre de 2016. Se aceptarán comentarios y/o discusiones hasta cinco meses después de su publicación.

⁽¹⁾ Research Assistant, Institute of Engineering, UNAM, Mexico, e-mail: hectorguerrerob@hotmail.com

⁽²⁾ Senior Lecturer, The University of Manchester, UK, e-mail: tianjian.ji@manchester.ac.uk

⁽³⁾ Professor, Institute of Engineering, UNAM, Mexico, e-mail: jess@pumas.iingen.unam.mx

intensidad sísmica que el caso sin CRP. Al final de las pruebas, los CRP fueron removidos y el modelo regreso a su posición original sin daño.

Palabras clave: contraventeos restringidos al pandeo (CRP); pruebas de vibración libre; pruebas en mesa vibradora; modelo de marco de acero; zona del lago de la Ciudad de México

INTRODUCTION

Mexico City, especially in the lakebed zone, possesses higher levels of seismic risk than many other cities around the world. This is reflected in the return periods for earthquake design which are lower than those in other standards, i.e. the equivalent return period for design in some zones of Mexico City is as low as 125 years (Reinoso and Jaimes, 2005; Rosenblueth et al., 1988). Structures located in these zones are likely to be subjected to large ductility demands during earthquakes, due to the characteristics of the ground motions of the very soft soil (Bojórquez and Ruiz, 2004, Arroyo and Ordaz, 2007, Teran-Gilmore and Bahena, 2008). The use of passive dissipation technology (like BRBs), in such structures, will help to effectively reduce the levels of seismic risk and their lifecycle costs, while increasing their reliability (Montiel and Teran-Gilmore, 2011).

Buckling-restrained braces (BRBs) are a type of passive seismic dissipater and represents one of the major developments in seismic design in recent years. Although there are several configurations (as summarised by Xie, 2005), it commonly consists of a rectangular steel core and a case (Figure 1). The core is weaker in the central zone so that the plastic deformations under cyclic loading are concentrated there. The case is often made either of a steel tube filled with concrete (e.g. Merrit et al., 2003; and Black et al., 2004), or all made of steel (e.g. Della Corte et al., 2014; and Formisano and Mazzolani, 2015). The function of the case is to prevent buckling of the core so that the device has similar capacity in tension and compression (Figure 1d). An unbounding material is located between the core and the case to avoid direct interaction. Several enhancements to BRBs have been proposed recently in order to improve their implementation in practical applications (e.g. Iwata and Murai, 2006; Zhao et al., 2010).

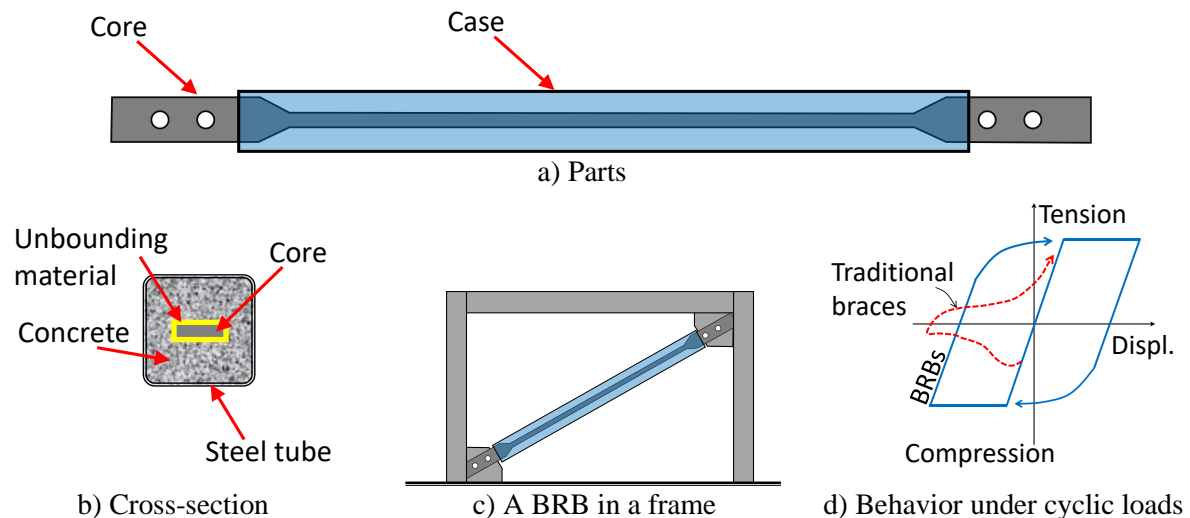


Figure 1. Buckling-Restrained Braces (BRBs)

Experimental tests on buckling restrained braces (BRBs), as isolated members, have demonstrated that these devices possess high energy dissipation capacity by means of stable and symmetric hysteretic loops when they are subjected to cyclic loads, e.g. (Merrit et al., 2003; Black et al., 2004; Uang and Nakashima, 2004; Iwata and Murai, 2006; Zhao et al., 2010). However, experiments are still needed in order to corroborate their good behaviour when located in actual building frames subjected to seismic loads. Unfortunately, most of the current studies have been conducted under quasi-static loading (e.g. Della Corte et al., 2014; and Formisano and Mazzolani, 2015). Although valuable information has been obtained, experiments under dynamic loads are desirable. In this regard, shaking table tests are significant because they allow assessing the dynamic behaviour of structures under conditions similar to those found in actual earthquakes (Benavent-Climent and Escolano-Margarit, 2012). Unfortunately, the number of such tests is still limited and conducted under particular types of seismic excitation. For example, Vargas and Bruneau (2009) tested a three-storey one-bay steel model, in a scale of 1/3, equipped with BRBs under a synthetic record on a shaking table in the USA. Under that synthetic record, the frame presented stable performance when the BRBs were introduced. Reductions of the lateral displacements and inter-storey drifts by 70% and an increment of the damping ratio, from 2% to 5%, were appreciated. Kasai et al. (2010) tested a full-scale five-storey steel building frame equipped with four different types of dampers (including BRBs) on a shaking table in Japan. The frame was subjected to the Takatori ground motion of the 1995 Kobe earthquake. Under such ground motion, they showed that the inclusion of dampers reduced the displacements, storey shears and absolute floor accelerations. They reported that the damping ratio remained unchanged when the model was subjected to low-intensity white noise input, with and without BRBs. However, for seismic input, an increase of the damping ratio, from 2% in the bare model to about 9% in the equipped structure, was reported. It was also observed that the damping ratio increased with the seismic intensity. Hu et al. (2010) tested a full-scale pinned-connected steel frame equipped with BRBs under the El Centro ground motion. They found that the BRBs performed well under a high seismic level motion; drift demands were well controlled and no damage was encountered in the structural elements of the frame. Hence they recommend the use of BRBs in seismic zones.

From the literature review, it is appreciated that past shaking table studies have been conducted for particular types of excitations. These specific conditions may not allow generalisation of the results. Therefore, it is of interest to assess the behaviour of structures equipped with BRBs subjected to low-frequency ground motions, such as those recorded in the lakebed zone of Mexico City, because this system may constitute an alternative to help to reduce or mitigate damages observed in the past in this region of the World.

This paper presents the results of shaking table tests of a five-storey building model equipped with BRBs undertaken in Mexico. The tests were focused on assessing the performance of a model frame when subjected to ground motions which are appropriate for the lakebed zone of Mexico City. In the following sections, the test setup of the studied model and the main results, from the free vibration and shaking table tests using white noise and seven actual seismic records, are presented. The results demonstrate the advantages of fitting these devices in buildings, because the response parameters (namely: lateral displacements, inter-storey drifts, floor velocities, floor accelerations, and energy contents) were all significantly reduced. It is highlighted that the experiments were conducted on a shaking table at the Institute of Engineering of the National Autonomous University of Mexico (UNAM).

TEST SETUP FOR THE FRAME BUILDING MODEL

The model

The one-tenth scale model building, as shown in Figure 2, has a height of 1450 mm, a width of 600 mm and a depth of 300 mm. It is composed of five storeys and is made of ASTM A-36 steel – which has nominal and expected yielding stresses of 250 MPa and 282 MPa, respectively, as reported by Merrit et al. (2003). The cross-sections of the members are given in Table 1. Since the main objective of the tests was to protect the main frame, the structural elements (beams and columns) were designed to remain elastic, while all nonlinear response was concentrated in the BRBs. More details of the design are described later. Two mass scenarios were considered: 1) 150 kg/m² on the floors one to four and 145 kg/m² on the fifth floor; and 2) 417 kg/m² on the floors one to four and 412 kg/m² on the fifth floor.

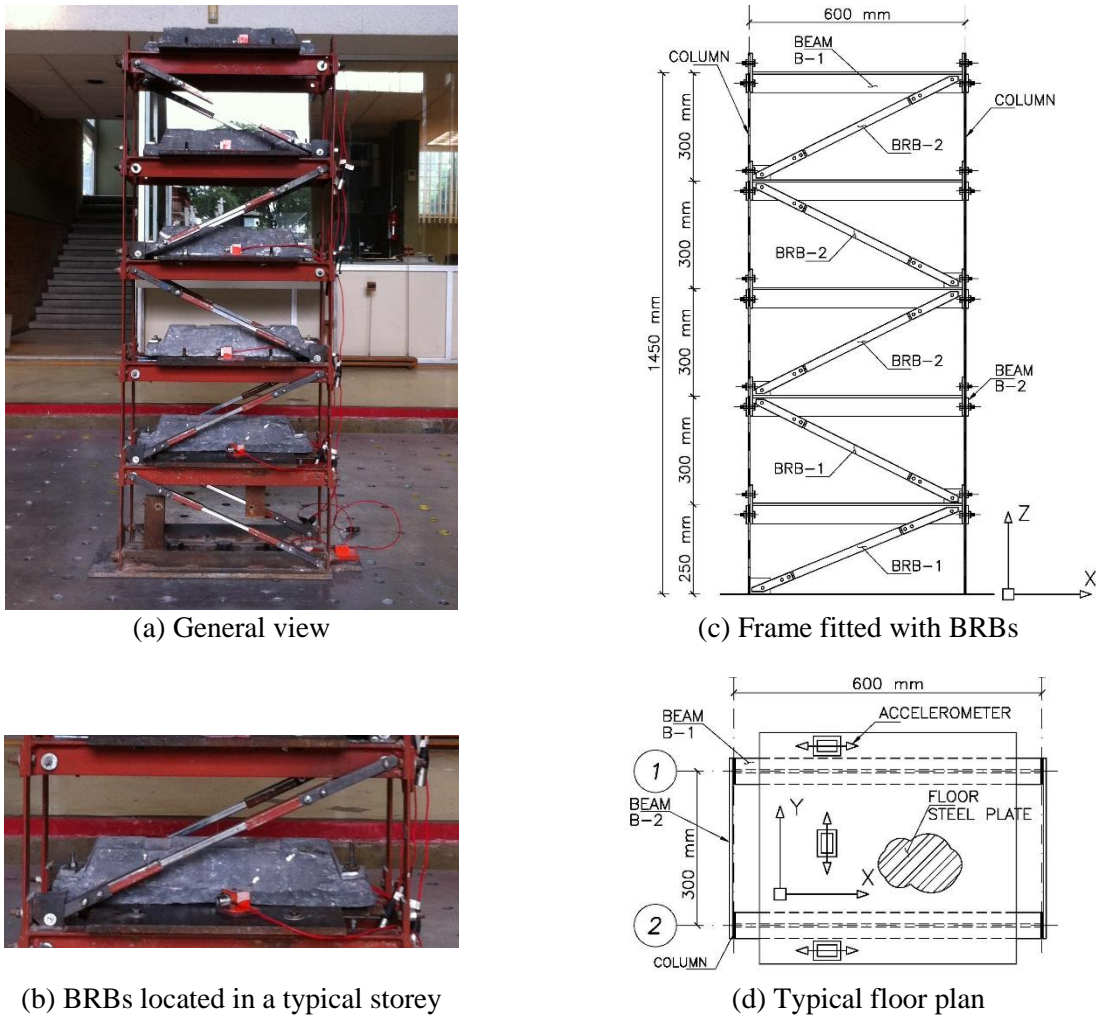


Figure 2. Building model

Table 1. Cross-sections of the structural elements

Structural Element	Profile	Cross-sectional area	Second moment of area
--------------------	---------	----------------------	-----------------------

Columns	Rectangular	243.84 mm ²	468.17 mm ⁴
Beams B-1 (X direction)	Tee	660.67 mm ²	207,685 mm ⁴
Beams B-2 (Y direction)	Rectangular	303.60 mm ²	64,777 mm ⁴

BRBs used in the tests

Due to the scale of the test frame model (1/10), there are no commercially available BRBs. Therefore, they had to be fabricated specifically for this study. The composition and dimensions of a typical BRB used in this study are shown in Figure 3.

Each BRB consists of a soft galvanised steel core, an encasing sleeve and two connection ends. The core steel had a yielding stress and elasticity modulus of $f_y=405$ MPa and $E_s=118,725$ MPa, respectively, obtained from laboratory tests. The core was wrapped with 0.2 mm polytetrafluoroethylene (PTFE) film, as unbonding material, to separate the core and mortar of the case. The two ends of the core were placed and fixed in the connection ends – which consist of two steel tubes and an epoxy material.

It is significant to mention that: a) the filling material consisted of a cement and sand mortar in proportion of 1:2 – which has an approximated resistance of 15 MPa; b) the epoxy material consisted of a mixture of an epoxy resin and a catalyst – which reaches a tensile resistance of 40 MPa; and c) the steel tubes of the case and the connection ends were square cross-sections of 13 mm x 13 mm and 19 mm x 19 mm, respectively, with wall thickness of 1 mm. Note that the cross-section of the case is smaller than that of the connection ends, in such a way that the connection tubes can cover a part of the case in order to avoid out-of-plane deformation of the BRBs.

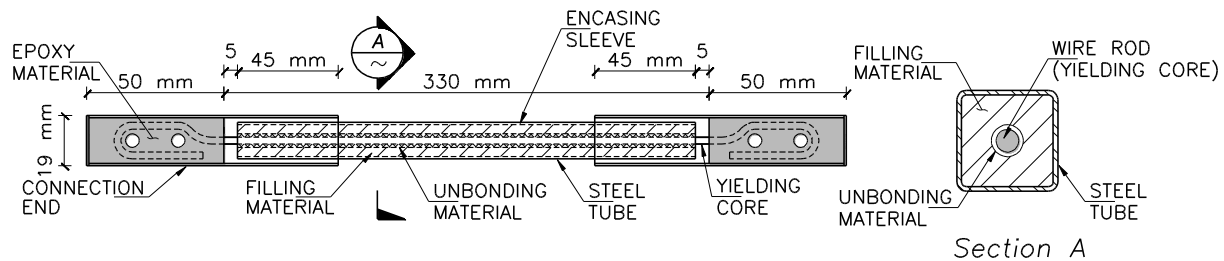


Figure 3. Schematic configuration of the BRBs used in the tests

The cross-sections of the cores were circular wire rods with diameters of: 1.6 mm (for BRBs type 1 used in the first two storeys.); and 1.2 mm (for BRBs type 2 used in the next three storeys). While more details of their design are described in the next section, the experimental response of a simple BRB type 1, as isolated member subjected to quasi-static sinusoidal displacement-controlled tests with amplitude of 0.5 mm, 1.0 mm and 2.0 mm, is shown in Figure 4. While quasi-elastic behaviour is observed for a displacement amplitude of 0.5 mm, slightly nonlinear response is observed for a displacement amplitude of 1.0 mm, and highly nonlinear behaviour of seen for 2.0 mm. These observations will be further discussed later.

On the other hand, the connections of the BRBs to the structure consisted of gusset plates, of ASTM A-36 steel, fastened with bolts. Two splice plates were used to connect each BRB end to each gusset plate. To join them, four 6.4 mm diameter bolts were used. In this case, the splice plates possessed large cross-sectional areas (60 mm² each), to avoid unexpected failures in the connections before the cores of the BRBs yielded.

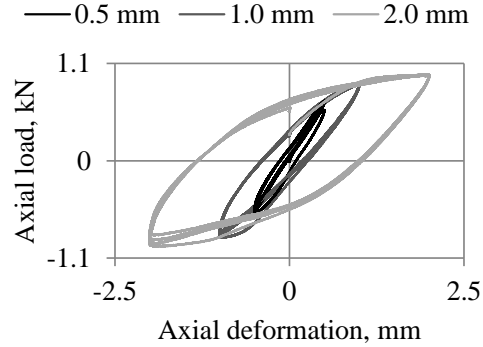


Figure 4. Experimental response of an isolated BRB under cyclic loads

Design of the BRBs

First, the capacity of the bare frame model was determined. Then, the BRBs were designed to increase the stiffness and lateral resistance of the model.

From a pushover analysis, and using the expected properties of the materials, the lateral resistance of the bare frame, normalised by its total weight (for the second mass scenario), was estimated to be $V_y/W=0.18$. Also, from eigenvalue analysis, its period of vibration was $T=0.31$ s - which according to the similitude laws (presented in the next section) corresponds to a full-scale period of $T=0.31\sqrt{10}=0.98$ s.

Since the period was considered long, and the strength low, for typical five-storey buildings located in the lakebed zone of Mexico City, BRBs were provided to the model. The design method proposed by Guerrero et al. (2016), which is based in the control of the lateral displacements, was applied. After a few iterations, it was observed that BRBs with cross-section areas of 2 mm^2 (in storeys one and two) and 1.1 mm^2 (in storeys three to five) provided satisfactory control of the lateral response while the main frame remained within its elastic deformation range. Note that the cross-sections areas correspond to the diameters of 1.6 mm and 1.2 mm described in the previous section. The final period of vibration of the equipped model resulted $T=0.22$ s (or 0.70 s in full scale) and the normalised strength was $V_y/W=0.38$. It is seen that the BRBs increased the lateral capacity by $0.20W$.

Similitude laws

As previously highlighted, the scale of the test model was 1/10 due to restrictions of cost and capacity of the test equipment. Therefore, similitude laws were developed using the theory of modelling (Harris and Sabnis, 1999). They are listed in Table 2. As an example, it is observed that the physical quantities of distance and displacement have a scale factor of 10 to go from the tested model to full scale and a factor of 1/10 to go from full scale to the tested model scale. Similarly, the period and time step have factor of $\sqrt{10}$ and $1/\sqrt{10}$, respectively.

Table 2. Similitude laws of the experiment

Physical property	Scale factor (from model to full-scale)	Scale factor (from full-scale to model)
Distance	10	1/10
Area	10^2	$1/10^2$
Second moment of area	10^4	$1/10^4$
Mass per area	1	1
Elasticity modulus	1	1
Stress	1	1
Period of vibration	$\sqrt{10}$	$1/\sqrt{10}$
Time step	$\sqrt{10}$	$1/\sqrt{10}$
Displacements	10	1/10
Velocities	$\sqrt{10}$	$1/\sqrt{10}$
Acceleration	1	1

Instrumentation and measured data

Three accelerometers were located on each floor: two in the longer direction (X) and one in the shorter direction (Y) (Figure 2d). Thus the responses in the X and Y direction and in the torsional direction could be monitored. Setra 141 accelerometers were used because of their high accuracy, output stability and measurement range (from static to 3000 Hz). The lateral displacements at each storey were estimated by double integration of the measured accelerations. To avoid unintended errors during the integration process, recommendations by Boore and Bommer (2005) were considered. No filtering, filtering between 0.1 and 20 Hz and between 0.5 and 20 Hz were tested. Figure 5a shows the 5%-damped elastic displacement spectra based on the accelerations recorded at the base of the model in one test. It is observed that none of the band-pass filters affected the response in the frequency range of interest between 1 Hz and 10 Hz. On the other hand, Figure 5b shows the transfer functions between the top floor and the base of the model, due to a white noise input. It shows that the band-pass filter between 0.5 Hz to 20 Hz eliminated the noise at low frequencies. Therefore, this filter was considered adequate, and errors in the estimation of the lateral displacements due to filtering may be considered negligible (Hudson, 1979). However, it is not possible to estimate permanent (or residual) displacements.

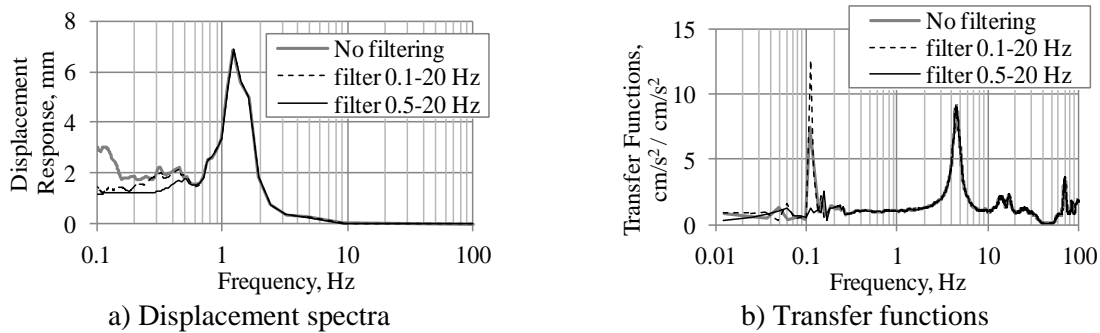


Figure 5. Determination of filter cut-offs

Seismic Input

Seven earthquake records were used to test the model (see Table 3). All seven were recorded in the lakebed zone of Mexico City, which is characterised by very soft soils, and they have dominant periods of

vibration around two seconds. The time step on each record was scaled by a factor of $1/\sqrt{10}$, according to the similitude laws developed for this model (see Table 2).

Table 3. Selected records for the tests

Record	Station	Date	Magnitude	Epicentral Distance (km)	<i>pga</i> (cm/s ²)
SCT-1	SCT1	19/09/1985	8.1	425	161.63
SCT-2	SCT2	25/04/1989	6.5	311	39.98
SCT-3	SCT2	14/09/1995	7.3	344	32.21
SCT-4	SCT2	15/06/1999	7.0	219	30.47
SCT-5	SCT1	15/06/1999	7.0	219	29.90
SCT-6	SCT1	30/09/1999	7.6	444	20.37
SCT-7	SCT2	20/03/2012	7.5	355	33.90

Design of the experiment

The input was applied in the longer direction of the model and in the orientation of the BRBs. The tests are summarised in Table 4 and described below:

In the first stage, the model with the first mass scenario was used for free vibration tests. An initial displacement was applied and then suddenly released to generate free vibration. The model without BRBs was first tested. Then, BRBs were introduced in the first storey and a free vibration test was conducted again. This was repeated until all five storeys of the model were fitted with BRBs. Finally the model was shaken using a (50 cm/s² RMS) white noise in order to measure its dynamic properties in an alternative manner. Reduced levels of mass were used at this stage to avoid unexpected damage to the model and elements.

Table 4. Summary of the test programme

Test type	Objective	Test	Description	Mass scenario	
Free vibration		1a	Bare frame (see Figure 5a)	1	
	Damping effects due to BRBs	2a	Frame with BRBs in 1 st storey (Figure 5b)	1	
		3a	Frame with BRBs up to 2 nd storey (Figure 5c)	1	
		4a	Frame with BRBs up to 3 rd storey (Figure 5d)	1	
		5a	Frame with BRBs up to 5 th storey (Figure 5e)	1	
Shaking table tests	Dynamic properties and damping	1b	White noise in bare frame (Figure 5a)	1	
		2b	White noise in full-equipped frame (Figure 5e)	1	
		3b	White noise in bare frame (Figure 7a)	2	
		4b	White noise in full-equipped frame (Figure 7b)	2	
	Responses to <i>PGA</i> = 0.1g	1c to 7c	Bare frame subjected to records SCT-1 to SCT-7 for <i>PGA</i> = 0.1g (Figure 7a)	2	
		8c to 14c	Full-equipped frame subjected to records SCT-1 to SCT-7 for <i>PGA</i> = 0.10g (Figure 7b)	2	
		Responses to higher <i>PGAs</i>	1d to 7d	Full-equipped frame subjected to records SCT-1 to SCT-7 for <i>PGA</i> = 0.15g (Figure 7b)	2
			8d to 14d	Full-equipped frame subjected to records SCT-1 to SCT-7 for <i>PGA</i> = 0.20g (Figure 7b)	2
			15d to 17d	Full-equipped frame subjected to records SCT-1 to SCT-3 for <i>PGA</i> = 0.25g (Figure 7b)	2

In the second stage, the model with the second mass scenario was used. The model was subjected to (50 cm/s^2 RMS) white noise. Then, seven ground motion records were applied at the base, with seismic intensities of: $pga = 0.10g, 0.15g, 0.20g$ and $0.25g$, respectively. For the intensity of $0.10g$, the model was tested with and without BRBs. For the other pga values, the model was fully equipped with BRBs in all storeys. Floor accelerations were measured in all tests. Then, the effects of the BRBs in the model were analysed.

Figure 5 shows the model used in the first stage of the tests and how the BRBs were gradually added to the model. Figure 7 shows the model with added mass (Mass scenario 2) in the second stage of the tests. The purpose of having the increased mass was: 1) to provide more realistic levels of mass; 2) to produce a longer fundamental period of vibration which generates larger displacements; and 3) to ensure that the BRBs go beyond their elastic limit to dissipate energy.

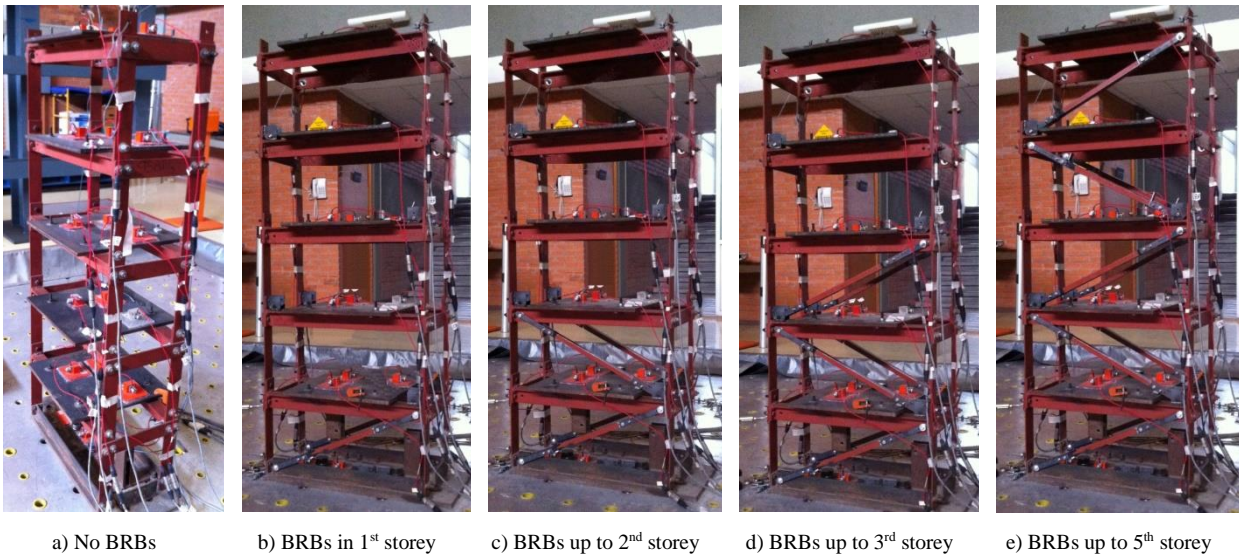


Figure 6. Model during the first stage of the tests

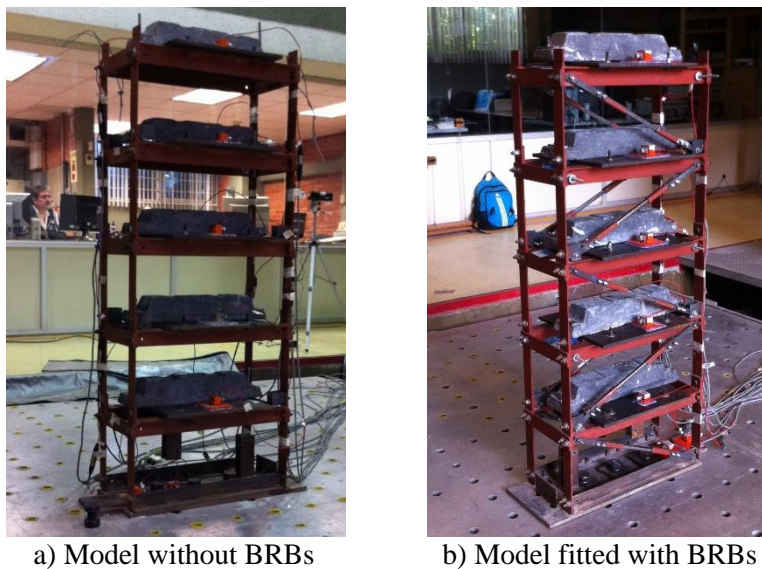


Figure 7. Model during the second stage of the tests

EXPERIMENTAL RESULTS

Free vibration tests

Figure 8 shows the recorded accelerations at the top floor for tests 1a to 5a, as described in Table 4 and shown in Figure 5. It can be observed that the vibration of the model decayed quickly due to the contribution of BRBs. This was due to an increase in the damping and stiffness of the model structure.

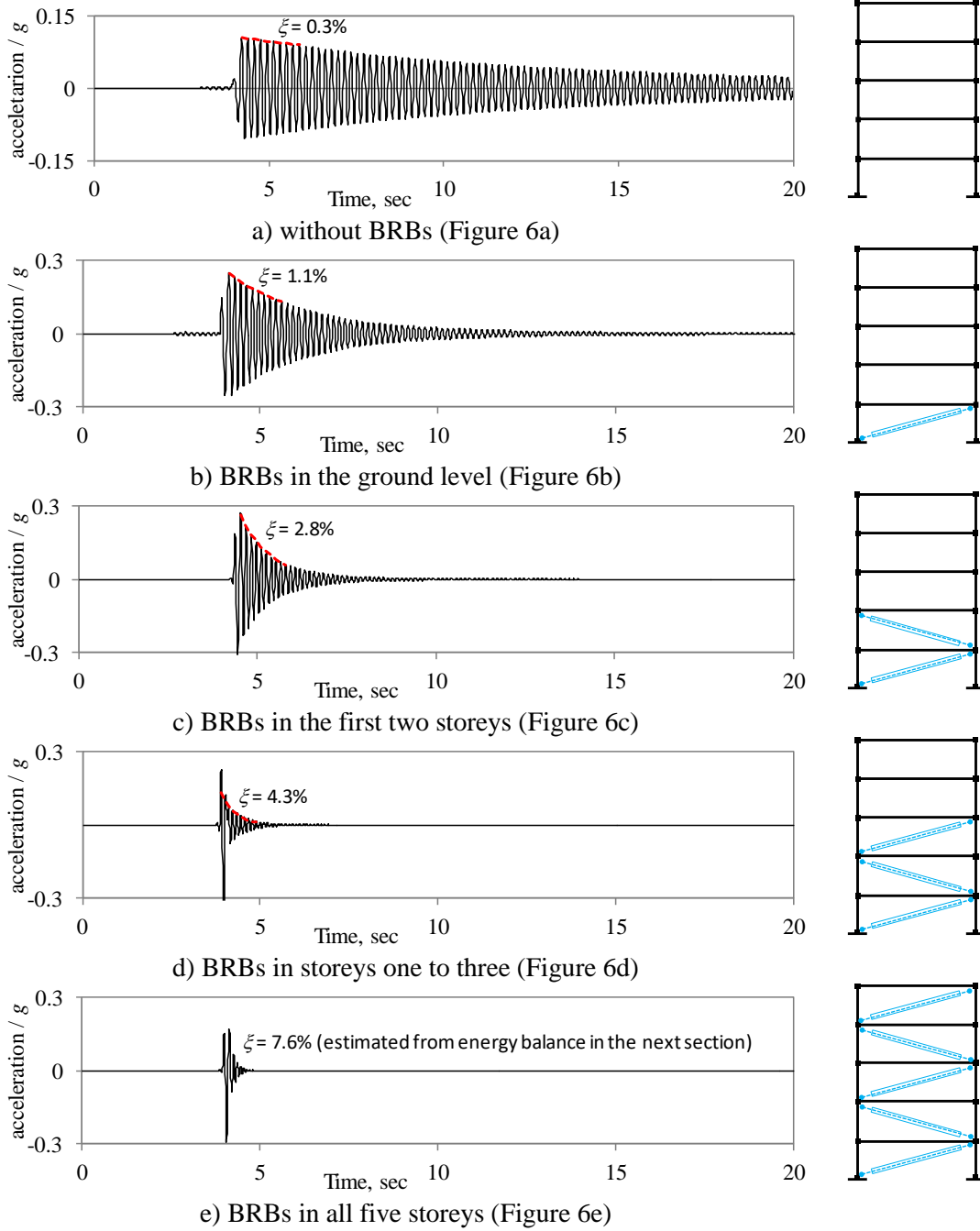


Figure 8. Measured accelerations at the top floor for the five bracing cases

The damping ratios for the first four cases were estimated by curve fitting to the first 10 oscillations of the measured data. For the last case, a white noise had to be induced in the model and the damping was estimated by balancing the damping energy equation (see next subsection). Figure 9a shows the damping ratio estimated for each case, in which the horizontal axis shows the number of pairs of BRBs used and the vertical axis the damping ratio. Similarly, Figure 9b shows the peak inter-storey drift demand for each pair of BRBs. It is observed that the inter-storey drift demands remained well below the yielding limit of 0.005, which is described later in Section “Inelastic behaviour of the BRBs”.

It is clear that the BRBs increased the damping significantly in the model and that the BRBs remained within their linear-elastic range. This is in agreement with observations by Vargas and Bruneau (2009). This finding may be significant because it is commonly assumed that BRBs do not provide damping when working in their linear range. However, it should be recognised that more experimental work is needed to validate the phenomenon shown in Figure 9 and the factors affecting these increments. Such experiments are under development and the results will be available.

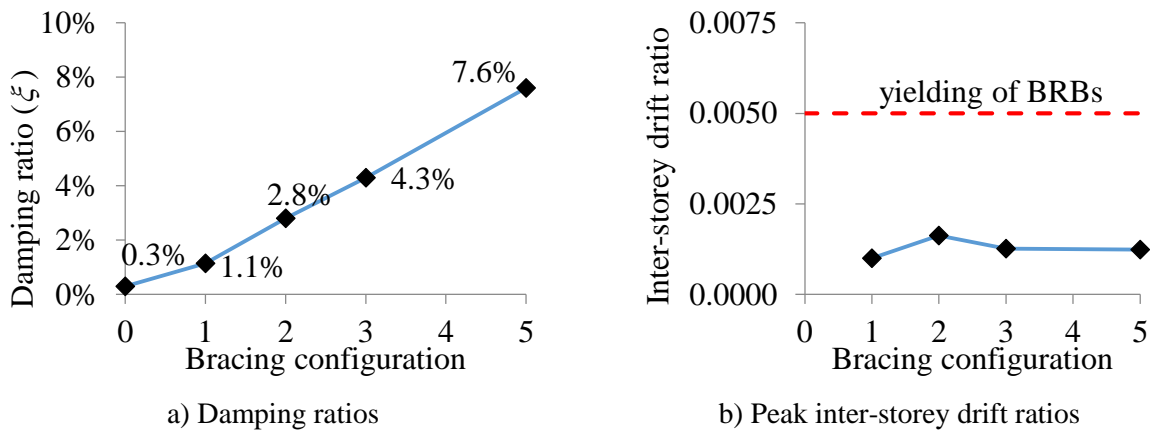


Figure 9. Damping and inter-storey drift ratios estimated for different BRB configurations

Shaking table tests with white noise input

Figure 10 shows the Transfer Functions (TF) of the Fourier spectra obtained for the tests 1b, 2b, 3b and 4b, which are summarised in Table 4. These tests included the two mass scenarios and the model with and without BRBs. The TF were obtained using the programme Degtra (Ordaz and Montoya, 2005) and the accelerations measured at the base and at the top floor of the model.

The fundamental frequencies and first-mode damping ratios are indicated in Figure 10. Two important facts are noted in this figure: 1) for both scenarios of mass, the frequencies increased when the BRBs were introduced; in other words, the BRBs increased the stiffness of the model; and 2) the spread of TFs became wider when BRBs were included in the model, indicating that the model fitted with BRBs possessed higher damping. The damping ratio increased from 0.3% to 7.6% for the first mass scenario, and from 0.52% to 6.10% for the second mass scenario. Again, this is in agreement with observations by Vargas and Bruneau (2009). However, it contradicts the findings by Kasai et al. (2010) for tests under white noise motions.

Now, it was recognised that the source of damping in the model structure was not viscous damping (Lazan, 1968, Charney, 2008). Thus an approach similar to that proposed by Blandon and Rodriguez (2007) was adopted. This approach recognises that equivalent viscous damping ratios may vary during the whole response time-history. Therefore, the equivalent damping ratios (ξ_{eq}) are expressed as (Chopra, 2012):

$$2\xi\omega m \int [\dot{u}(t) / \Gamma_1]^2 dt = - \int m \ddot{u}_g(t) [\dot{u}(t) / \Gamma_1] dt - \frac{1}{2} m [\dot{u}(t) / \Gamma_1]^2 - \frac{1}{2} m \omega^2 [u(t) / \Gamma_1]^2 \quad (1)$$

where m is the modal mass, ω is the angular frequency of vibration, \ddot{u}_g is the acceleration at the base, Γ_1 is the first-mode participation factor, and \dot{u} and u are the relative velocity and displacement at the top floor of the model.

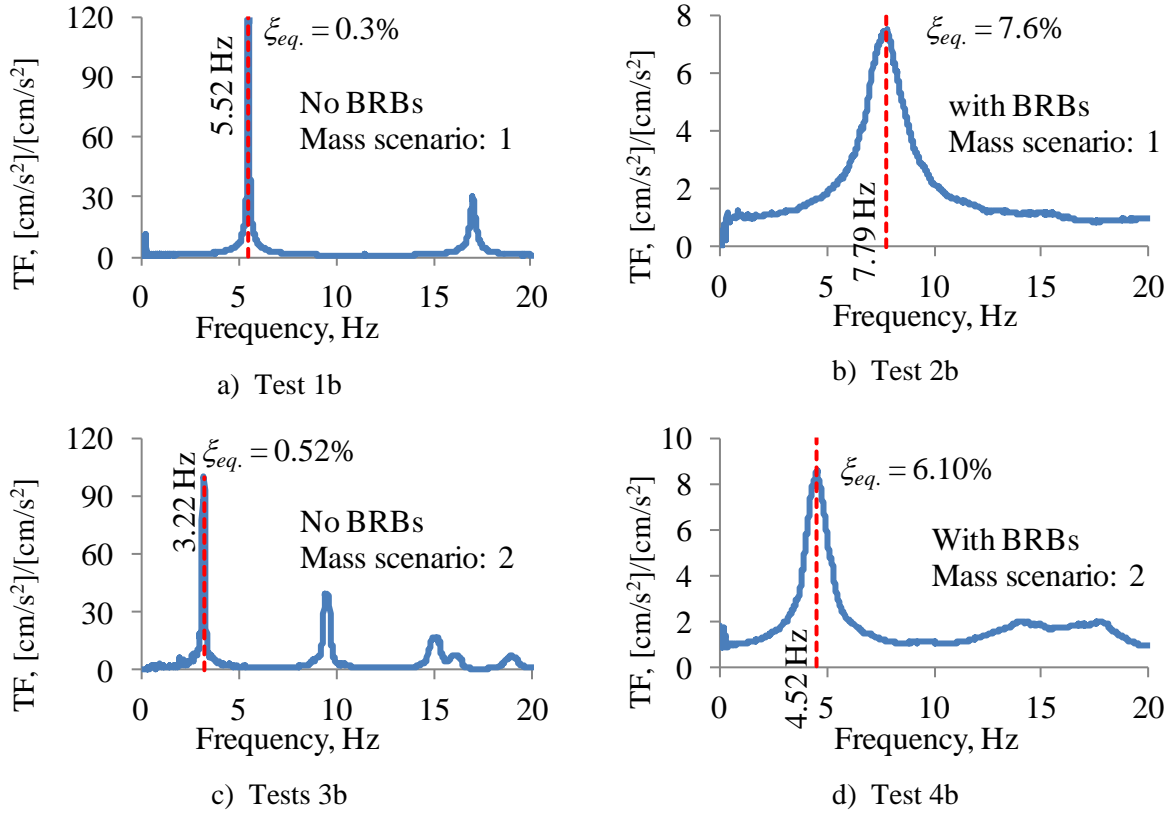


Figure 10. Transfer Functions (from the top floor to the base) for the test model

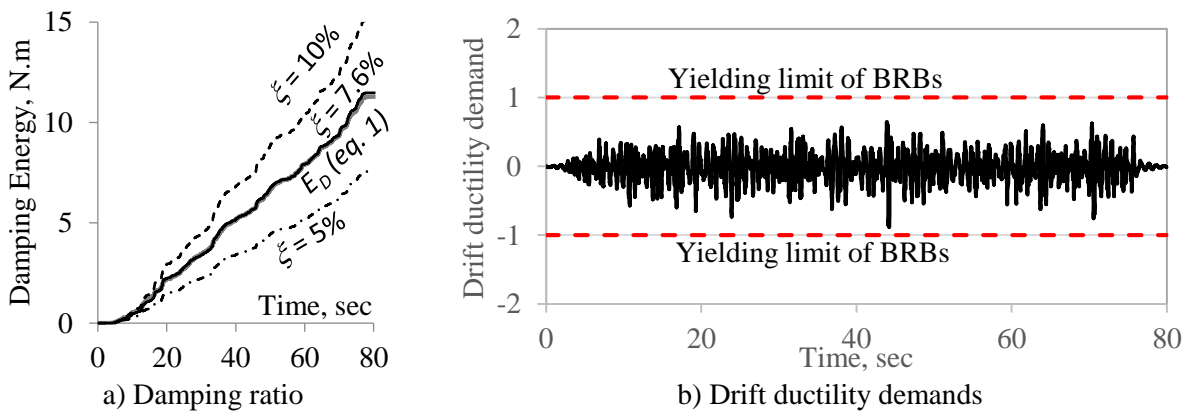


Figure 11. Estimation of equivalent viscous damping ratio for test 2b

Since all parameters of equation (1), except ξ_{eq} , can be readily estimated using the measured floor accelerations, an equivalent ξ_{eq} can be determined by minimising the difference between the left and right sides of the equation. As an example, Figure 11a shows the damping energy (in the time domain) estimated for the test 2b using equation 1. Damping ratios of $\xi = 5\%$, 7.6% and 10% were used in the left side of the equation (see the dark lines). As observed, the value of $\xi = 7.6\%$ balances the damping energy estimate with the right side of the equation (see the grey line). Therefore, this value is considered as the equivalent viscous damping ratio for the model for this particular case. All other viscous damping ratios in Figure 10 were estimated in the same way. To verify that the structure remained within its linear-elastic response during test 2b, the drift ductility demand, defined as the ratio of the inter-storey drift demands to the yielding drift ratio of $\theta_y=0.005$ (which is calculated later in Section “Inelastic behaviour of the BRBs”), was determined. The drift ductility demands are shown in Figure 11b, where it is seen that the ductility demands remained below the yielding point of unity.

Shaking table tests with seismic input

The results are presented in two parts: 1) comparison of the responses on the frame model with and without BRBs for a seismic intensity of $pga=0.1g$; and 2) response of the model fully-equipped with BRBs subjected to incremental seismic intensity (i.e. for $pga=0.10g$, $0.15g$, $0.20g$ and $0.25g$).

Response at Peak Ground Acceleration (pga) of 0.1g

The response of the models with and without BRBs are compared considering five parameters: 1) lateral relative displacements, 2) inter-storey drifts; 3) absolute floor velocities; 4) absolute floor accelerations; and 5) Arias intensity (Arias, 1970) (I_a), relative to the base.

Figure 12 shows only the response of the models with and without BRBs measured at the top floor of the model subjected to SCT-2. It can be observed that the response reduced when BRBs were included in the model. The average reductions for the five parameters were evaluated. The average reduction of the maximum lateral displacement at the top floor was 58.5% ; the average reduction of the maximum inter-storey drifts was 62.2% . This effect may be expected in structures located on soft soils, because the model became stiffer and had higher damping when the BRBs were included. The average reductions of the maxima values of the floor velocities and floor accelerations were 35.4% and 26.9% , respectively. The reductions in floor velocities and accelerations is an important finding in this study, because this contradicts some numerical studies which suggested that BRBs generally increase these parameters (e.g. see (Kelly, 2008)). On the other hand, even when the reductions of the maxima values of displacements, inter-storey drifts, floor velocities and accelerations are significant, it would be of interest to compare the response in terms of energy content in order to have an alternative measure of the expected damage. Therefore, the Arias intensity (I_a) (Arias, 1970), as a measure of energy content in the movement, was estimated for the acceleration at the top floor relative to the base (Figure 13). On average, the ratio of the Arias intensities for the model without BRBs to that with BRBs was 7.93 . This suggests that the expected damage to the structure without BRBs might be significantly larger than the damage to the structure fitted with BRBs. It can also be seen in Figure 13 that the ending of the intense phase ($95\% I_a$) was earlier when BRBs were included.

Response to higher values of pga

To examine the effect of the seismic intensity on the model fitted with BRBs, the intensity was increased from $pga=0.1g$ to $0.25g$, in increments of $0.05g$ for the seven records. During the tests, two local failures were observed in the BRBs. The first was observed when the SCT-1 record, scaled to $pga = 0.20g$, was applied. The BRB at the south side of the third storey broke. Both BRBs of the third storey (which were

type 2) were replaced by BRBs type 1 and the tests continued. The second partial failure occurred at the north side of the third storey, when the SCT-3 record, scaled to $pga = 0.25g$, was applied. The test programme was interrupted at that stage.

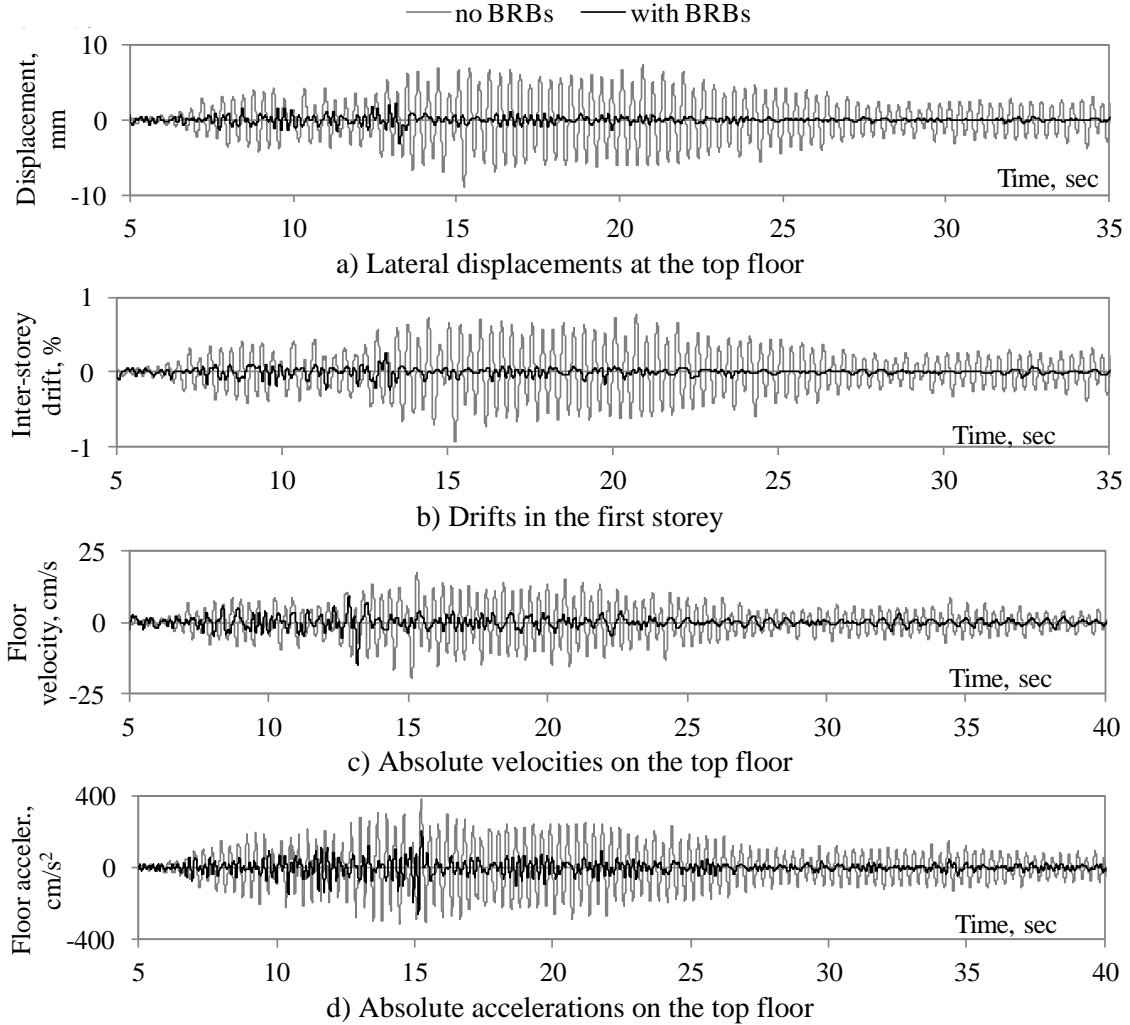


Figure 12. Responses of the test model (with and without BRBs) for $pga=0.1g$ and record SCT-2

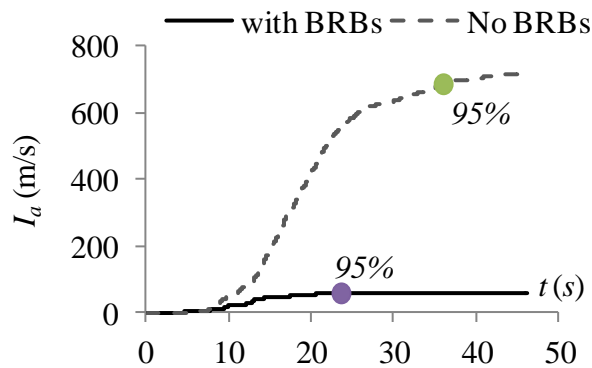


Figure 13. Arias intensity at the top floor, relative to the base, for tests 2c and 9c

Figure 14a, c, d and e show the maximum values of displacement, floor velocity, floor acceleration and 95% of the relative Arias intensity at the top floor, while Figure 14b shows the maximum inter-storey drift. The duration of Arias Intensity is presented in Figure 14f. All the parameters were estimated for the four intensity levels and the seven seismic records. The averages of the responses are shown by a thick dark line in the figure. The maximum responses of the model without BRBs, subjected to the seven seismic records at $pga = 0.10g$, are also shown in Figure 17 for comparison.

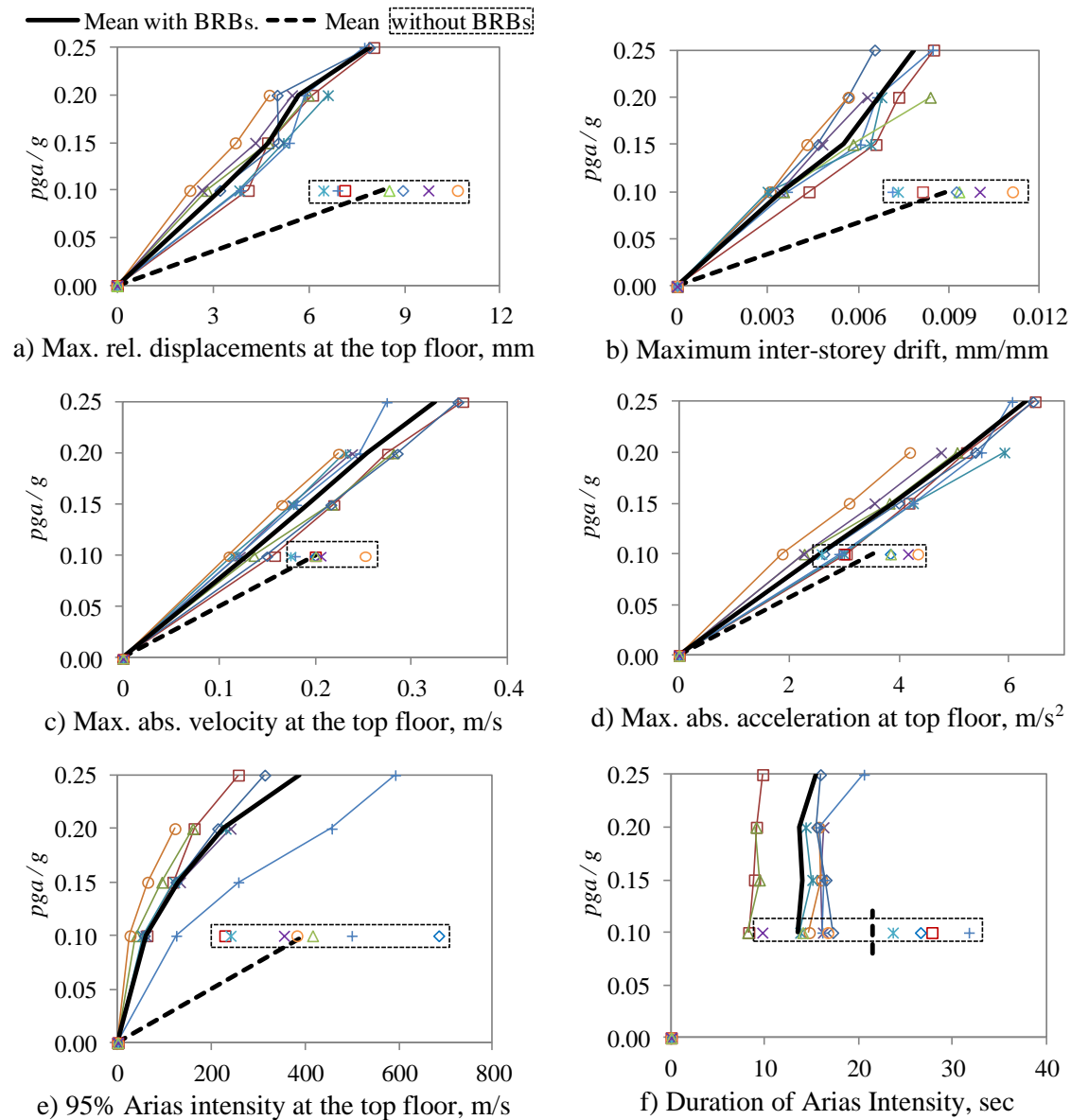


Figure 14. Maximum responses of the test model subjected to incremental seismic intensity

It can be observed, from Figure 14, that the inclusion of BRBs significantly reduced the responses. The mean of the maximum displacements, maximum inter-storey drifts and the Arias Intensity of the model equipped with BRBs and subjected to an intensity of $pga = 0.25g$, were smaller than that for the model without BRBs subjected to $pga = 0.1g$. For the floor velocities and floor accelerations, the model with

BRBs can accommodate about 1.5 times more seismic intensity than the model without BRBs. In addition, by observing the dispersion of the data, it is appreciated that the model with BRBs is less sensitive to the seismic input than the bare model at the intensity level of $pga=0.1g$.

Finally, the duration of the intense phase (from $0.05I_a$ to $0.95I_a$), provided in Figure 14f, shows that the model fitted with BRBs had a much shorter duration of the intense phase. When the model was equipped with BRBs, the durations of the intense phases of the Arias intensities were almost constant for all four values of pga and the average duration was less than that on the bare model for $pga = 0.10g$.

Inelastic behaviour of the BRBs

This section is developed to determine the seismic intensity at which the BRBs reached inelastic behaviour, i.e. the seismic intensity at which the BRBs started dissipating energy by plastic deformation of their steel core.

First, the yielding inter-storey drift (θ_y) is estimated and then compared to the maxima demands of Figure 14b. θ_y is defined by:

$$\theta_y = \frac{\Delta_y}{h} = \frac{u_y}{\cos \alpha} \frac{1}{h} \quad (2)$$

where Δ_y is the relative displacement between two consecutive storeys at which yielding of the BRBs is expected, u_y is the BRBs axial deformation at which they yield, α is the inclination angle of the BRBs, and h is the inter-storey height.

By considering the connection ends of the BRBs used in the experiment as infinitively stiff, the yielding deformation of the BRBs can be estimated as:

$$u_y = \varepsilon_y L_y = \frac{f_y}{E_s} L_y \quad (3)$$

where L_y is the yielding length of the steel core of the BRBs, and f_y and E_s are the material's yielding stress and modulus of elasticity – which were determined experimentally.

Substituting the values of $L_y=330$ mm (see Figure 3) and the experimental values of $f_y=405$ MPa and $E_s=118,725$ MPa. The yielding deformation of the BRBs is $u_y=1.12$ mm. This is in agreement with the results of Figure 4 – where slightly nonlinear behaviour was appreciated for displacement deformation around 1 mm or below. Substituting $u_y=1.12$ mm in equation (2) the yielding inter-storey drift in the first storey, where the maxima demands were observed, is:

$$\theta_y = \frac{1.12}{0.923} \frac{1}{250} = 0.005$$

By comparing $\theta_y = 0.005$ with the inter-storey drift demands of Figure 14b, it can be observed that the BRBs presented linear-elastic behaviour for a seismic intensity of $pga=0.10g$, while inelastic behaviour started at an intensity of $pga=0.15g$.

DISCUSSION

The measured results indicate that the model equipped with BRBs reduces the responses and their record-to-record variability (and hence, uncertainties). In addition, the Arias intensity (as a measure of the energy contents) showed that the model with BRBs may present significantly less damage than the model without BRBs.

Increases in damping were observed due to the inclusion of BRBs in the model. The damping increased from 0.3% to 7.6% for the first mass scenario and from 0.52% to 6.1% for the second mass scenario. However, it is difficult to quantify the contributions from the BRBs and from the connections between BRBs and the model. The observed increases of damping are significant and should be considered in the design process of structures equipped with BRBs. Depending on the design approach, namely force-based design (FBD) or displacement-based design (DBD), the level of damping provided by BRBs can be included straightforwardly. For example, in the FBD approach the increase of damping can be considered by modifying the design spectrum with a correction factor, such as that defined by equation (3.6) of Eurocode 8 (2004). In the DBD approach, the increased damping ratio can be considered directly in the estimation of the displacement demands, e.g. in equation (10) by Guerrero et al. (2016) the damping ratio provided by the BRBs (ξ_2) can be added to the damping ratio provided by the primary structure (ξ_1).

The permanent (or residual) deformations of the model equipped with BRBs were not possible to measure during the tests. But no permanent deformations were visually identified after each test and after all the BRBs were removed. This gives an indication of the low permanent deformation of the tested model. The costs associated with rehabilitation of structures equipped with BRBs may be reduced to replacing the devices without interruptions to the building functionality; which may be regarded as a cost-effective solution.

Since the responses of the model equipped with BRBs were significantly improved, it may be thought that these devices would benefit structures located in the lakebed zone of Mexico City. Including BRBs in new designs could lead to better performance or lower construction costs. Also existing buildings could be upgraded to achieve enhanced levels of performance.

CONCLUSIONS

Free vibration and shaking table tests have been carried out on a five-storey model and the results are summarised in this paper. The following conclusions have been reached:

1. The inclusion of BRBs in the model not only increased the stiffness but also the damping. For the first and second scenarios of mass, the increases were from $\xi=0.3\%$ to 7.6% and from $\xi=0.52\%$ to 6.10%, respectively.
2. All the response parameters (and record-to-record variability) were reduced for the model fitted with BRBs. Using the same $pga=0.1g$, the average values of the maximum displacement and maximum inter-storey drift were reduced by 58.5% and 62.2%, respectively. The maximum floor velocities and maximum floor accelerations were reduced by 35.4% and 26.9%, respectively. The Arias Intensity, as a measure of the energy content, was almost eight times less on the structure with BRBs than on the structure without BRBs.
3. These reductions suggest that structural and non-structural damage and losses of contents may be significantly less when BRBs are included in structures located in the lakebed zone of Mexico City.
4. From the tests with incremental seismic intensity, it can be concluded that the model fitted with BRBs was able to accommodate up to 2.5 times more seismic intensity in terms of lateral displacements, inter-

storey drifts and Arias Intensity, and up to 1.5 times more seismic intensity in terms of floor velocity and floor acceleration.

5. Residual deformations of the model were not visually identifiable before or after all the BRBs were removed from it.

ACKNOWLEDGEMENTS

The first author recognises the sponsorship provided by CONACyT, SEP and UNAM from Mexico.

REFERENCES

- Arias, A (1970), “A Measure of Earthquake Intensity” In: Hansen, R J (ed.) *Seismic Design for Nuclear Power Plants*, MIT Press, Cambridge, Massachusetts, USA.
- Arroyo, D and M Ordaz (2007), “Hysteretic Energy Demands for SDOF Systems Subjected to Narrow Band Earthquake Ground Motions. Applications to the Lake Bed Zone of Mexico City”, *Journal of Earthquake Engineering*, 11, 147-165. [DOI:10.1080/13632460601123131](https://doi.org/10.1080/13632460601123131)
- Benavent-Climent, A and D Escolano-Margarit (2012), “Shaking table tests of structures with hysteretic dampers: experimental results versus prediction using non-linear static methods”, *Bulletin of Earthquake Engineering*, 10, 1857-1883. [DOI:10.1007/s10518-012-9375-6](https://doi.org/10.1007/s10518-012-9375-6)
- Black, C J, N Makris and I D Aiken (2004), “Component testing, seismic evaluation and characterization of buckling-restrained braces”, *Journal of Structural Engineering*, ASCE, 130, 880–894. [DOI:10.1061/\(ASCE\)0733-9445\(2004\)130:6\(880\)](https://doi.org/10.1061/(ASCE)0733-9445(2004)130:6(880))
- Blandón, J J and M E Rodríguez (2007), “Estudio analítico-experimental y propuesta de diseño sísmico de sistema de pisos rígidos en edificios”. *Serie Investigación y desarrollo*, Instituto de Ingeniería - UNAM.
- Bojórquez, E and S E Ruiz (2004), “Strength Reduction Factors for the Valley of Mexico, Considering Low-Cycle Fatigue Effects”. *13th WCEE*. Vancouver, B.C., Canada.
- Boore, D M and J J Bommer (2005), “Processing of strong-motion accelerograms: needs, options and consequences”. *Soil Dynamics and Earthquake Engineering*, 25, 93-115. [DOI:10.1016/j.soildyn.2004.10.007](https://doi.org/10.1016/j.soildyn.2004.10.007)
- Charney, F A (2008), “Unintended Consequences of Modeling Damping in Structures”. *Journal of Structural Engineering*, ASCE, 134, 581-590. [DOI:10.1061/\(ASCE\)0733-9445\(2008\)134:4\(581\)](https://doi.org/10.1061/(ASCE)0733-9445(2008)134:4(581))
- Chopra, A K (2012), “Dynamics of Structures: Theory and Applications to Earthquake Engineering”, 4th Edition, Prentice Hall, Englewood Cliffs, New Jersey.
- Della Corte, M, D'aniello R and Landolfo (2015), “Field testing of all-steel buckling-restrained braces applied to a damaged reinforced concrete building”, *Journal of Structural Engineering ASCE*, 141 (1), p D4014004. [DOI:10.1061/\(ASCE\)ST.1943-541X.0001080](https://doi.org/10.1061/(ASCE)ST.1943-541X.0001080)
- Eurocode 8 (2004), “Eurocode 8: Design of structures for earthquake resistance. Part 1: General rules, seismic actions and rules for buildings”, Ref. No. EN 1998-1:2004: E.
- Formisano, A and F M Mazzolani (2015), “On the selection by MCDM methods of the optimal system for seismic retrofitting and vertical addition of existing buildings”, *Computers and Structures*, 149, pp. 1-13. [DOI:10.1016/j.compstruc.2015.06.016](https://doi.org/10.1016/j.compstruc.2015.06.016)

- Guerrero, H, T Ji, A Teran-Gilmore and J A Escobar (2016), “A method for preliminary seismic design and assessment of low-rise structures protected with Buckling-Restrained Braces”. *Engineering Structures*, 123, pp. 141–154. [DOI:10.1016/j.engstruct.2016.05.015](https://doi.org/10.1016/j.engstruct.2016.05.015)
- Harris, H G and G M Sabnis (1999), “Structural modelling and experimental techniques”, Second Edition, CRC Press.
- Hu, D, G Li, F Sun, D Wang, M Rui, L Li and J He (2010), “Full-scale shaking table tests on a hinge-connected steel frame with buckling restrained braces”. *China Civil Engineering Journal*, 43, 520-525.
- Hudson, D E (1979), “Reading and Interpreting strong motion accelerograms”, *Earthquake Engineering Research Institute*, Berkeley, CA.
- Iwata, M and M Murai (2006), “Buckling-restrained brace using steel mortar planks; performance evaluation as a hysteretic damper”, *Earthquake Engineering and Structural Dynamics*, 35, 1807–1826. [DOI:10.1002/eqe.608](https://doi.org/10.1002/eqe.608)
- Kasai, K, H Ito, Y Ooki, T Hikino, K Kajiwara, S Motoyui, H Ozaki and M Ishii (2010), “Full-Scale Shake Table Tests of 5-Story Steel Building with various Dampers”. *Joint Conference 7CUEE & 5ICEE*, Tokyo Institute of Technology, Tokyo, Japan.
- Kelly, T E (2008), “Improving Seismic Performance: Add Stiffness or Damping?”, *Bulletin of the New Zealand Society for Earthquake Engineering*, 41, 24-30.
- Lazan, B J (1968), “Damping of materials and members in structural mechanics”, *Pergamon Press*, Oxford, UK.
- Merrit, S, C M Uang, and G Benzoni (2003), “Subassemblage testing of Corebrace Buckling-Restrained Braces”, *Report No. TR-2003/04*, University of California, San Diego, La Jolla, CA.
- Montiel, M and A Teran-Gilmore (2011), “Comparative reliability of two 24-story braced buildings: traditional versus innovative”, *The structural design of tall and special buildings*, 22 (8), 635-654. [DOI:10.1002/tal.716](https://doi.org/10.1002/tal.716)
- Ordaz, M and C Montoya (2005), “Degtra v5.1.0”, *Institute of Engineering, UNAM*, Mexico City, Mexico.
- Reinoso, E and M Jaimes (2005), “Accelerograms for building design for hard soil in Mexico City”, *Earthquake Resistant Engineering Structures*, 81, 23-32. [DOI:10.2495/ERES050031](https://doi.org/10.2495/ERES050031)
- Rosenblueth, E, F M Sanchez-Sesma, y S K Singh (1988), “Design spectra for Mexico's Federal District”, *9th WCEE*, Tokyo, Japan.
- Teran-Gilmore, A and N Bahena (2008), “Cumulative ductility spectra for seismic design of ductile structures subjected to long duration motions: Concept and theoretical background”, *Journal of Earthquake Engineering*, 12, 152-172. [DOI:10.1080/13632460701364486](https://doi.org/10.1080/13632460701364486)
- Uang, C M and M Nakashima (2004), “Steel Buckling-Restrained Braced Frames”. In: Bozorgnia, Y & V V Bertero (editors) *Earthquake Engineering from Engineering Seismology to Performance-Based Engineering*. *CRC Press*.
- Xie (2005). “State of the art of buckling-restrained braces in Asia”, *Journal of Constructional Steel Research*, 61 (6), 727–748. [DOI:10.1016/j.jcsr.2004.11.005](https://doi.org/10.1016/j.jcsr.2004.11.005)
- Vargas, R and M Bruneau (2009), “Experimental Response of Buildings Designed with Metallic Structural Fuses. II”, *Journal of Structural Engineering-ASCE*, 135, 394-403. [DOI:10.1061/\(ASCE\)0733-9445\(2009\)135:4\(394\)](https://doi.org/10.1061/(ASCE)0733-9445(2009)135:4(394))

Zhao, J, B Wu and J Ou (2011), “A novel type of angle steel buckling-restrained brace: cyclic behaviour and failure mechanism”, *Earthquake Engineering and Structural Dynamics*, 40, 1083–1102.
[DOI:10.1002/eqe.1071](https://doi.org/10.1002/eqe.1071)